Cancer Research

Dll4 Blockade in Stromal Cells Mediates Antitumor Effects in Preclinical Models of Ovarian Cancer

Frank Kuhnert, Guoying Chen, Sandra Coetzee, Nithya Thambi, Carlos Hickey, Jing Shan, Pavel Kovalenko, Irene Noguera-Troise, Eric Smith, Jeanette Fairhurst, Julian Andreev, Jessica R. Kirshner, Nicholas Papadopoulos, and Gavin Thurston

Abstract

The Notch ligand delta-like 4 (Dll4) has been identified as a promising target in tumor angiogenesis in preclinical studies, and Dll4 inhibitors have recently entered clinical trials for solid tumors, including ovarian cancers. In this study, we report the development of REGN421 (enoticumab), a fully human IgG1 monoclonal antibody that binds human Dll4 with sub-nanomolar affinity and inhibits Notch signaling. Administering REGN421 to immunodeficient mice engineered to express human Dll4 inhibited the growth of several human tumor xenografts in association with the formation of nonfunctional tumor blood vessels. In ovarian tumor xenograft models, Dll4 was expressed specifically by the tumor endothelium, and Dll4 blockade by human-specific or mouse-specific Dll4 antibodies exerted potent antitumor activity, which relied entirely on targeting Dll4 expressed by tumor stromal cells but not by the tumor cells themselves. However, Dll4 blockade reduced Notch signaling in both blood vessels and tumor cells surrounding the blood vessels, suggesting that endothelial-expressed Dll4 might induce Notch signaling in adjacent ovarian tumor cells. The antitumor effects of targeting Dll4 were augmented significantly by simultaneous inhibition of VEGF signaling, whereas this combined blockade reversed normal organ vascular changes induced by Dll4 blockade alone. Overall, our findings deepen the rationale for antibody-based strategies to target Dll4 in ovarian cancers, especially in combination with VEGF blockade. *Cancer Res; 75(19); 4086–96.* ©*2015 AACR.*

Introduction

The Notch pathway is an evolutionary conserved signaling system that regulates cell fate specification and tissue patterning (1). In mammals, the Notch signaling system consists of five canonical membrane-bound ligands, Dll (delta-like) 1, 3, 4, and Jagged 1 and 2, and four single-pass transmembrane receptors, Notch1-4. Ligand binding to the extracellular domain of Notch triggers the proteolytic activation of the receptor and translocation of the Notch intracellular domain (NICD) to the nucleus, where it interacts with CSL (CBF1, Suppressor of Hairless, Lag-1) transcription factor to regulate the expression of Notch target genes (2).

Functional studies have demonstrated a critical role for Dll4-Notch signaling during the formation of the vascular system (3–5). Dll4-Notch signaling functions downstream of VEGF and acts as a negative regulator of endothelial cell proliferation and sprouting, in part by downregulating the expression of VEGF receptors (6–12). In preclinical tumor models, blockade of Dll4-Notch signaling results in the formation of hypersprouting, nonfunctional tumor vasculature, associated with the inhibition of tumor growth (13–16).

Unlike γ-secretase inhibitors that broadly block all Notch signaling, specific pharmacologic targeting of Dll4 with anti-Dll4 antibodies does not induce overt gastrointestinal toxicity and has thus emerged as an attractive target for antiangiogenic cancer therapy (15, 17). Indeed, anti-Dll4 antibodies have recently entered clinical trials for the treatment of advanced solid tumors, including ovarian malignancies. In human tumors, Dll4 expression is typically restricted to the tumor vasculature, and low to undetectable in the vasculature of adjacent normal tissue (13, 18–22). In breast and ovarian cancer, Dll4 expression appears correlated to clinical outcome (18, 23).

Angiogenesis plays an important role in ovarian physiology and cancer biology, and the exploration of VEGF-targeting agents in this disease has demonstrated clinical benefit (24). However, not all ovarian cancers are responsive to VEGF inhibitors (25), and initially sensitive tumors eventually develop resistance to VEGF inhibitors (26, 27). Thus, there is great clinical need to target additional antiangiogenic pathways to increase clinical benefit. Here, we examined the activity of a new potent and specific antibody inhibitor of Dll4-Notch signaling, REGN421 (called enoticumab), in ovarian xenograft models. We demonstrate potent antitumor activity of Dll4 blockade in ovarian tumor xenograft models that is dependent on targeting stromal Dll4. In addition to the effect of REGN421 treatment on tumor angiogenesis, we identified spatially restricted, paracrine Dll4-Notch signaling interactions, which may promote ovarian tumor growth. The antitumor activity of Dll4 blockade in ovarian tumors was markedly augmented by the simultaneous targeting of VEGF signaling while normal organ vascular changes

Regeneron Pharmaceuticals, Inc., Tarrytown, New York.

Note: Supplementary data for this article are available at Cancer Research Online (http://cancerres.aacrjournals.org/).

Current address for I. Noguera-Troise: Merck & Co, Inc., Kenilworth, New Jersey.

Corresponding Author: Frank Kuhnert, Regeneron Pharmaceuticals, 777 Old Saw Mill River Rd, Tarrytown, NY 10591. Phone: 914-847-5498; Fax: 914-345-7544; E-mail: frank.kuhnert@regeneron.com.

doi: 10.1158/0008-5472.CAN-14-3773

AACR

induced by Dll4 blockade alone are reversed, thus suggesting enhanced clinical benefit for this combination approach.

Materials and Methods

Generation of antibodies

VelocImmune mice (with genes encoding human immunoglobulin heavy and kappa light chain variable regions) were immunized with recombinant human Dll4 extracellular domain. Spleens were harvested for generation of hybridomas or for direct isolation of antigen-positive splenocytes. The cloned human immunoglobulin variable region genes from antibodies exhibiting the desired characteristics were joined to human IgG1 constant region genes for production in chinese hamster ovary (CHO) cells. REGN421 was selected as a lead antibody from more than 300 antigen-positive clones, based on *in vitro* biochemical properties as well as the ability to inhibit tumor xenograft growth.

Research grade, function-blocking antibodies to murine Dll4 (REGN1035), human/mouse Notch1, and Notch3 were generated using VelociImmune technology.

Determination of REGN421 binding affinity

Surface plasmon resonance (SPR)–based BiaCore technology was used to determine both on-rate and off-rate kinetic data to calculate an equilibrium dissociation constant for each of the antigen–antibody interactions. The binding specificity of REGN421 for Dll4 was evaluated using BiaCore-based SPR technology. The equilibrium dissociation constant (K_D) was mathematically calculated from the dissociation rate constant (kd) divided by the association rate constant (ka). REGN421 was analyzed for binding to recombinant soluble monomeric forms of human, monkey (Macaca fascicularis), and murine Dll4. In addition, binding kinetics of REGN421 to dimeric Fc-fusions of human and monkey Dll4 were also determined. The kinetic parameters were obtained by globally fitting the data to a 1:1 binding model using BiaEvaluation software 4.1.

Notch reporter assay

The ability of REGN421 to bind Dll4 was also evaluated in an ELISA format. Serial dilutions of antibodies were bound to microtiter plate–coated human Dll4 (fused with two myc epitope tags and 6XHis) for 1 hour at room temperature. Bound antibodies were detected with a horseradish peroxidase (HRP)–conjugated a-hIgG polyclonal antibody and developed with tetramethylbenzidine and analyzed in Prism. The EC_{50} value was calculated, defined as the concentration of REGN421 required to achieve 50% of Dll4 maximal binding signal. The ability of REGN421 to block human Dll4 binding to Notch1 was tested in a competition sandwich ELISA assay. Various concentrations of REGN421 or isotype control antibody were mixed with 30 pmol/L biotinylated extracellular domain of human Dll4 fused with the Fc portion of the human IgG1 protein and incubated for 1 hour at room temperature. The mixture was then transferred to a microtiter plate coated with hNotch1 (fused with human Fc) to capture the unbound Dll4 in the solutions. Plate-bound Dll4 was detected with HRP-conjugated streptavidin and developed with tetramethylbenzidine substrates. Data analysis was performed with Graphpad Prism software using a sigmoidal dose–response model, and IC_{50} values were determined (concentration of REGN421 required to block 50% of Dll4 binding). To determine the ability of REGN421 to neutralize Dll4-mediated cellular functions *in vitro*, an HEK293 cell line expressing human Notch 1 was stably transfected with a CBF1-luciferase reporter plasmid (28). Titration of the amount of coated Dll4 ligand established a dose-dependent response curve of reporter activation. Based on the observed dose response for plate-coated Dll4 ligand, the bioassay plates were coated with Dll4 at a concentration of 1 nmol/L at 16 hours prior to addition of the HEK293 reporter cells and REGN421. Cells were incubated at 37°C for 24 hours following which Dll4-mediated signaling was measured by quantitation of luciferase activity (shown in arbitrary units). A titration of varying concentrations of REGN421 was used to establish an inhibition curve, and an IC_{50} value of approximately 21 pmol/L was observed for inhibition of Dll4-mediated signaling by REGN421. TOV-112D cells were stably transduced with a RBPj-luc Notch signaling reporter construct (Qiagen). TOV-112D/RBPj-luc cells displayed luciferase expression in response to immobilized Dll4. To quantify Notch signaling inhibition, a fixed amount of biotinylated Dll4 was coated onto the streptavidin plate for 2 hours at room temperature, and monoclonal antibodies were preincubated with TOV112D/RBPj-luc cells for 1 hour before addition to the plates. After overnight incubation, luciferase activity was measured using the substrate ONE-Glo (Promega).

HUVEC fibrin bead sprouting assay

To assess the effects of REGN421 on three-dimensional endothelial cell growth *in vitro*, fibrin bead assay was performed (29). Briefly, Cytodex beads were coated with sub-confluent human umbilical vein endothelial cell (HUVEC) cells (Lonza) and embedded in fibrin gel. Lung fibroblasts were seeded on top of the gel, and antibodies were added at 25 μg/mL. Fresh antibodies were added with each EGM-2 medium change every 2 days. On day 7, HUVEC sprouts were fixed and processed as described (30). Maximum intensity projections of transmitted light Z-stacks were collected on Image Xpress Micro at 10×. MetaXpress Journal was used to quantitate the number of nuclei per bead (approximately 250 beads/well were analyzed). Branch points were quantitated manually (15 beads per well were analyzed).

FACS analysis

To determine Notch receptor expression in ovarian xenograft cell lines, cells were incubated with primary antibodies at 4°C for 30 minutes. Antibodies used were as follows: Notch1, Notch3 (generated at Regeneron), Notch2, and Notch4 (both Biolegend).

Generation of humanized Dll4 mice

Since REGN421 does not cross react with rodent Dll4, "humanized" mice were created in which the gene region encoding the Dll4 extracellular domain was replaced with the analogous DNA sequences encoding the human Dll4 extracellular domain via homologous recombination in ES cells. Resultant humanized Dll4 mice were phenotypically normal and fertile, indicating that extracellular human Dll4 can bind to mouse Notch receptors and functionally substitute for the mouse extracellular domain. For additional validation, the effects of the Dll4 humanization on thymus homeostasis were analyzed. Thymus size and gene expression profiles were essentially unchanged in humanized Dll4 mice relative to wild-type mice, while anti-Dll4 antibody treatment severely impaired thymic cellularity and T-cell differentiation with concomitant substantial gene expression changes, thus

further demonstrating that the humanization of Dll4 promotes normal Dll4-Notch signaling. The humanized Dll4 allele was crossed onto the immunodeficient SCID mouse strain to enable xenograft tumor studies.

Tumor xenograft growth studies

Tumor cells obtained from the ATCC (the identities of our human tumor cell lines were authenticated by short tandem repeat profiling at the ATCC) were implanted subcutaneously into the hind flank of 8- to 12-week-old humanized Dll4 or wild-type C.B.-17 SCID mice (for Colo205, HT1080, TOV-112D, SKOV-3, OVCAR-3, OV-90 tumors, 1×10^6 cells), or intraperitoneally (A2780, 2×10^6 cells). Once subcutaneous tumors were established (100–200 mm^3 in volume), mice were randomized into treatment groups ($n = 5$–8 mice per group) and injected subcutaneously with human Fc control protein, REGN421, REGN1035 (mouse Dll4-specific surrogate monoclonal antibody), or aflibercept at the indicated doses and treatment intervals. Fully effective doses of REGN421 and REGN1035 for once-weekly dosing were defined as 2.5 mg/kg and 5 mg/kg, respectively. Tumor size (in mm^3) was calculated from caliper measurements by using the formula for a spheroid approximation $4/3 \times \pi$ [length (mm)/2] $\times$ [width (mm)/2]^2, with width as the smaller dimension. Average tumor growth for each treatment group was compared using one-way ANOVA and Bonferroni multiple comparison test. For intraperitoneal A2780 tumor growth studies, treatment was initiated 1 or 2 weeks after tumor cell implantation, as indicated. In A2780 survival studies, demised animals found in a cage or intraperitoneal tumor burden exceeding 5 grams were defined as events. All procedures were conducted according to the guidelines of the Regeneron Institutional Animal Care and Use Committee.

PK modeling

The Michaelis–Menten model with parallel linear and nonlinear elimination was utilized to estimate pharmacokinetics of REGN421 in mouse. There were 2 physiologic compartments (injection site and central compartment) in the model. The differential equations from the primary model are described below:

$$\frac{d\Lambda_1}{dt} = -k_1\Lambda_1. \quad (1)$$

$$\frac{d\Lambda_2}{dt} = -k_e\Lambda_2 - \frac{\Lambda_2 V_m}{K_m + \frac{\Lambda_2}{V_2}} + k_a\Lambda_1, \quad (2)$$

where A_1 is the amount of functional REGN421 at the injection site, A_2 is the amount of functional REGN421 in the central compartment, k_e is the elimination rate, V_2/F is the apparent volume of central compartment, k_a is the first-order absorption rate constant, V_{max} is the maximum rate of target-mediated elimination, and K_m is the Michaelis–Menten constant. NONMEM version 6 was used for modeling and simulation.

Immunohistochemical analysis

Paraffin-embedded, formalin-fixed tumor sections were stained with a rat anti-murine CD31 (BD Pharmingen) following proteinase K-mediated antigen retrieval. Where applicable, sections were subsequently stained with Ki67 antibody (BD Pharmingen) to assess cellular proliferation. Notch1-ICD IHC staining was performed with cleaved Notch1-specific antibody (Cell Signaling Technology) as described (31), and samples were costained with anti-human vimentin antibody (Invitrogen) where applicable. For immunofluorescence (IF) staining, optimal cutting temperature (OCT)–embedded tumor sections were stained with antibodies to CD31 (Millipore), PDGFRβ (eBioscience), and human vimentin (Invitrogen). Where applicable, tumor microvascular density was quantified using NIH ImageJ software. IF and IHC staining for Dll4 expression was performed using a proprietary Regeneron Dll4 antibody. Notch1 expression in ovarian xenograft tumors was analyzed with rabbit anti-Notch1 antibody (Cell Signaling Technology). A2780 tumor perfusion was assessed by transcardiac FITC-lectin perfusion (50 mg Isolectin B4; Vector labs) followed by perfusion fixation with 1% paraformaldehyde and CD31IF staining of OCT-embedded tumor sections.

Results

Fully human monoclonal antibody, REGN421, binds human Dll4 with high affinity and inhibits endothelial Dll4-Notch signaling

Human antibodies against Dll4 were generated as described in Materials and Methods. The lead antibody REGN421 (selected from more than 300 antigen-positive clones) exhibited high-affinity binding to human and monkey Dll4, as measured in SPR Biacore experiments, but did not bind to murine Dll4 or human Dll1 and Dll3 (Supplementary Table S1 and data not shown). The equilibrium dissociation constants (K_D) for REGN421 binding to monomeric and dimeric Fc-fusion of human Dll4 were determined as 161 pmol/L and 5.1 pmol/L, respectively (Supplementary Table S1). K_D values for REGN421 binding to monkey Dll4 were 183 pmol/L and 5.85 pmol/L for monomeric and dimeric protein, respectively (Supplementary Table S1). The high similarity between the equilibrium dissociation constants of human and monkey Dll4 are consistent with the high sequence homology of these two proteins (98%). Epitope mapping revealed REGN421 binding to the junction of *N*-terminal and DSL domain within the Dll4 extracellular domain (data not shown).

In ELISA, REGN421 bound human Dll4 protein with an EC_{50} of 88 pmol/L and inhibited human Dll4 binding to Notch1 with an IC_{50} of 95.3 pmol/L (Fig. 1A and B). In cell-based assays, REGN421 blocked Dll4-mediated Notch signaling in dose-dependent manner with an IC_{50} of 21 pmol/L (Fig. 1C).

In addition, the ability of REGN421 to inhibit endogenous Dll4-Notch interactions was assayed in the HUVEC-based fibrin bead sprouting assay. REGN421 treatment resulted in a significantly increased number of branch points and endothelial cells per bead relative to control antibody (Fig. 1D). The induction of these hallmarks of impaired Dll4-Notch signaling in endothelial cells (9) demonstrates that REGN421 functions as a potent and specific inhibitor of Dll4-Notch signaling.

REGN421 potently inhibits tumor xenograft growth and induces aberrant tumor angiogenesis

To assess the effect of REGN421 on human tumor growth in preclinical xenograft models, humanized Dll4 (huDll4) SCID mice, in which the region of the mouse Dll4 gene encoding the extracellular domain were replaced with the equivalent region of the human Dll4 gene, were generated. Administration of REGN421 antibody (10 mg/kg, 3×/week) to huDll4 mice with established subcutaneous HT1080 (sarcoma) or Colo205 (colorectal) human

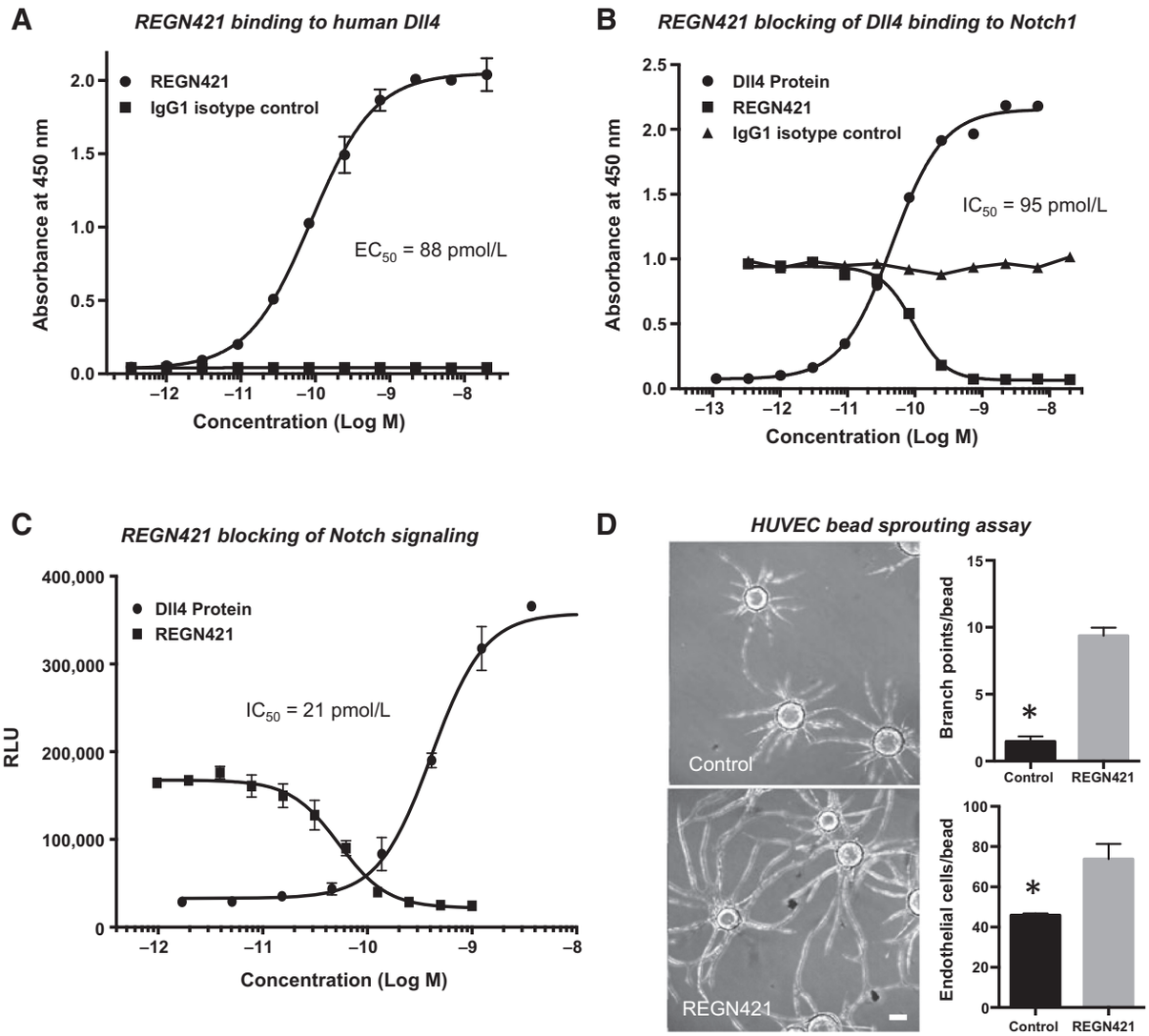

Figure 1.

REGN421 potently inhibits endothelial Dll4-Notch signaling. A, REGN421 at the indicated concentrations was added to plate-bound human Dll4. The EC_{50} for REGN421 binding to human Dll4 was determined as 88 pmol/L. B, the ability of REGN421 to block human Dll4 binding to Notch1 was tested in a competition sandwich ELISA assay. REGN421 (squares) inhibited human Dll4 binding to plate-coated Notch1 in dose-dependent manner with an IC_{50} value of 95 pmol/L. C, coating of Dll4 at the indicated concentrations established a dose-dependent response curve of Notch reporter activation (closed circles) with an EC_{50} of 360 pm. An IC_{50} of 21 pmol/L was observed for the inhibition of Dll4-mediated Notch signaling by REGN421 (open circles). D, the effects of REGN421 treatment on three-dimensional endothelial cell growth and sprouting were analyzed in the fibrin bead assay. Representative images of maximum intensity projections at ×10 magnification of transmitted light Z-stacks are shown on the left. REGN421 treatment resulted in significant increases in the number of branch points and endothelial cells per carrier bead relative to antibody control. Scale bar in D represents 100 μm.

tumors resulted in potent inhibition of tumor growth with 113% and 94% tumor growth inhibition (TGI), respectively (Fig. 2A). Notably, REGN421 is highly active in the HT1080 tumor model, which was previously demonstrated to be resistant to VEGF inhibition (14). Immunohistological analysis revealed dramatic changes in the tumor vasculature in both xenograft models (Fig. 2B), demonstrating that REGN421 is effective in xenograft tumor models with very different vascular morphologies.

To determine the effective dose range at which REGN421 inhibits HT1080 tumor growth, dose titrations were performed. Dose levels of REGN421 as low as 1 mg/kg administered twice weekly resulted in maximal inhibition of HT1080 tumor growth (114% TGI), with doses down to 0.3 mg/kg still producing significant antitumor effects (Fig. 2C). For once-weekly dosing regimens, a dose of REGN421 of 2.5 mg/kg was found to be maximally effective (Fig. 2D). Pharmacokinetic analysis of REGN421 in huDll4 mice showed evidence of target-mediated clearance (REGN421 half-life of 90 hours vs. 284 hours in huDll4 vs. wild-type mice) and indicated that doses of REGN421 achieving sustained circulating levels of $\geq$ 2 μg/mL correlated with maximal antitumor activity in the HT1080 model (Supplementary Fig. S1).

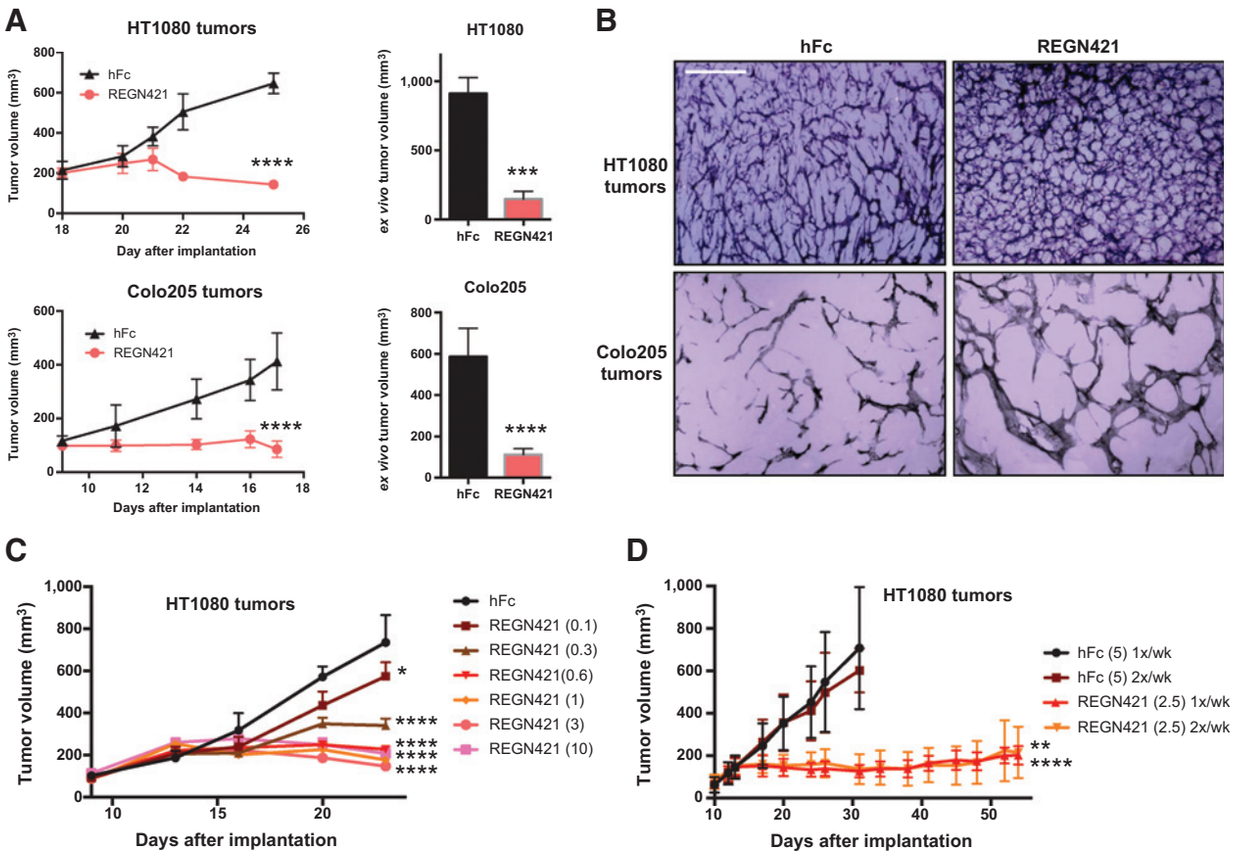

Figure 2.
REGN421 potently inhibits tumor xenograft growth and induces aberrant tumor angiogenesis. A, humanized Dll4 SCID mice bearing established HT1080 or Colo205 tumors were treated thrice weekly with human Fc control protein or REGN421 at 10 mg/kg. The line graphs depict the average tumor volumes over the course of treatment, whereas the bar graphs represent the *ex vivo* tumor volumes at the end of study. Error bars represent SEM. B, end of study tumors were sectioned and stained with an antibody to CD31 to visualize blood vessels. C, humanized Dll4 SCID mice bearing established HT1080 tumors were treated twice weekly with human Fc control protein or REGN421 at doses ranging from 0.1 to 10 mg/kg as indicated. D, comparison of anti-HT1080 tumor activity of once- and twice-weekly dosing of REGN421 at 2.5 mg/kg. Tumor growth curves and end of study tumor volumes in A, C, and D were compared with the Fc control group by 2-way ANOVA with the Bonferroni multiple comparison test (*, $P < 0.05$; **, $P < 0.01$; ***, $P < 0.001$; ****, $P < 0.0001$); error bars represent SEM. Scale bar in B represents 100 μm.

Potent antitumor activity of Dll4 blockade in ovarian xenograft models is dependent on targeting Dll4 in the stroma

Angiogenesis plays an important role in ovarian physiology and cancer, and antiangiogenic agents have demonstrated clinical benefit in this disease. Thus, we evaluated the activity of REGN421 in several ovarian xenograft models. REGN421 treatment (2.5 mg/kg, once weekly) of huDll4 mice bearing established intraperitoneal A2780 or subcutaneous TOV-112D, SKOV-3, or OV90 human xenografts resulted in tumor growth inhibition of 83%, 86%, 61%, and 55%, respectively (Fig. 3A and B; Supplementary Fig. S2). The inhibition of A2780 ovarian tumor growth by REGN421 was associated with a marked increase in tumor vascular structures but reduced vascular perfusion (Fig. 3C). To delineate the relative contributions of blocking stromal versus tumor cell expressed Dll4 to antitumor efficacy, we treated wild-type SCID mice bearing established intraperitoneal A2780 tumors with either REGN1035, selectively blocking murine Dll4, or with human Dll4-specific REGN421 to achieve selective targeting of host (mouse) versus tumor (human) Dll4. Potent A2780 tumor growth inhibition (70% TGI) was observed by strictly targeting stromal Dll4 with REGN1035 (at a fully effective dose of 5 mg/kg, 1×/week) in SCID mice (Fig. 3B). In contrast, the specific blockade of tumor cell–expressed human Dll4 did not exhibit any appreciable anti-A2780 tumor activity (Fig. 3B). Similarly, the targeting of stromal Dll4 with REGN1035 resulted in marked growth inhibition of subcutaneous TOV-112D (74% TGI), SKOV-3 (64% TGI), and OVCAR-3 tumors (84% TGI) and associated tumor vessel abnormalization. In contrast, the selective blockade of tumor cell Dll4 did not inhibit TOV-112D tumor growth (Supplementary Figs. S2 and S3). These findings are consistent with the restricted Dll4 expression in the tumor vasculature of ovarian xenograft tumors (Fig. 3D; Supplementary Fig. S4).

Paracrine Dll4-Notch signaling in ovarian xenograft tumors

The blockade of Dll4 results in potent antitumor effects in ovarian xenograft tumors; the degree of tumor growth inhibition, however, is variable between the different models. Thus, we investigated the possibility of paracrine signaling between

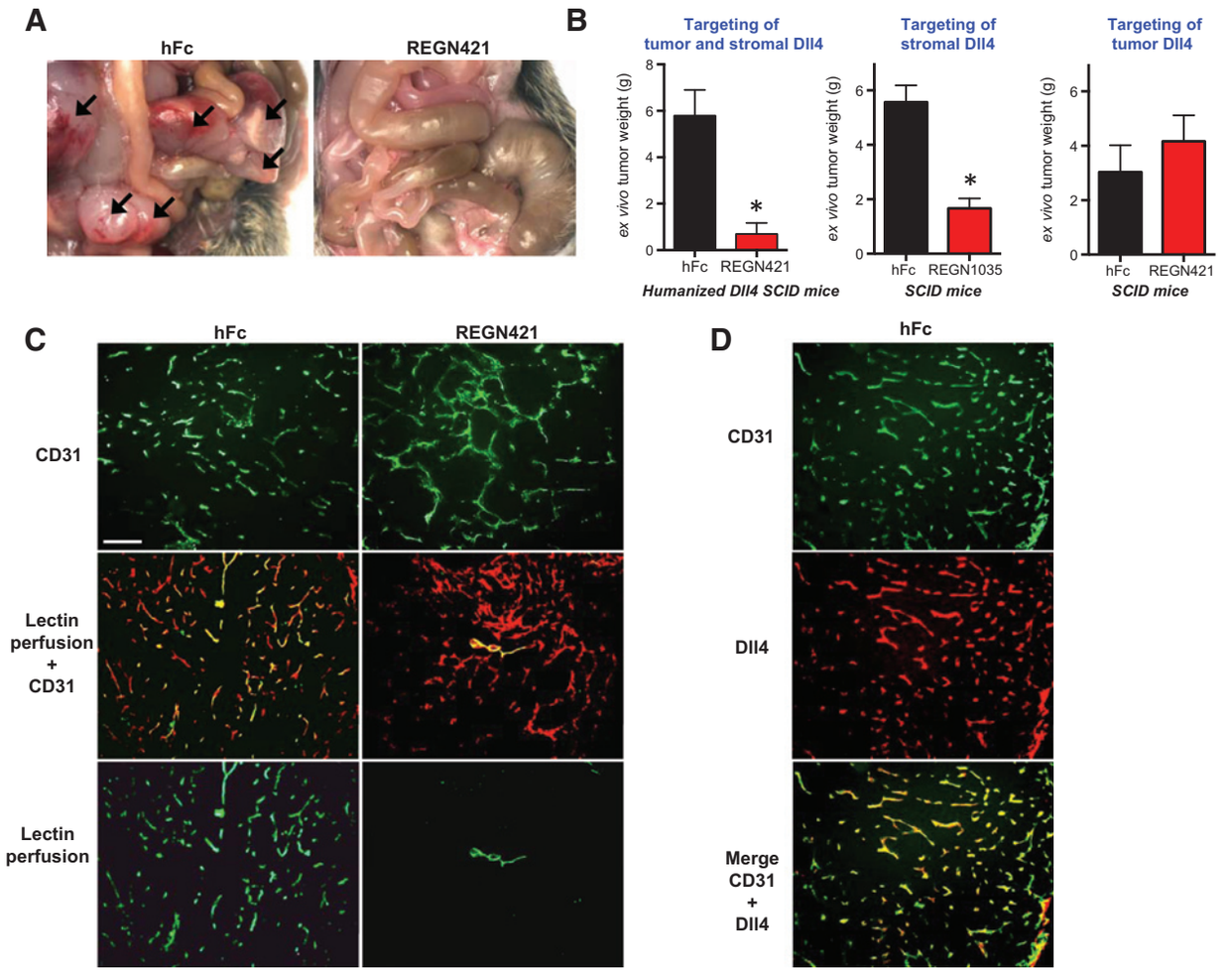

Figure 3.
The potent antitumor activity of Dll4 blockade in ovarian xenograft models is dependent on targeting Dll4 in the stroma. A, humanized Dll4 SCID mice bearing established intraperitoneal A2780 human xenograft tumors were treated once weekly with hFc or REGN421 at 2.5 mg/kg for 4 weeks. At the end of study, animals treated with hFc control protein exhibited multiple, large intraperitoneal A2780 tumors (arrows), whereas treatment with REGN421 quantitatively suppressed A2780 tumor growth. B, humanized Dll4 or wild-type SCID mice bearing established A2780 tumors were treated once weekly with human Dll4-blocking REGN421 (2.5 mg/kg) or with the mouse Dll4-specific blocker REGN1035 (5 mg/kg) versus hFc control protein to delineate the selective targeting of stromal versus tumor cell–expressed Dll4. Bar graphs represent end of study *ex vivo* tumor weight. Error bars represent SEM. Tumor weight was compared with the hFc control groups by unpaired *t* test (*, $P < 0.05$). C, immunohistochemical evaluation of microvascular density by CD31 staining in A2780 tumors implanted into humanized Dll4 SCID mice treated with hFc control protein or REGN421 (top panel). A2780 tumor perfusion was assessed by FITC-lectin perfusion followed by CD31 staining 72 hours after treatment. Loss of FITC (green) and CD31 (red) colocalization indicates loss tumor vessel perfusion (middle panel). Single FITC-lectin channel is shown in the bottom panel. Scale bar, 200 μm. D, immunohistochemical evaluation of Dll4 expression relative to CD31 in A2780 tumors implanted into humanized Dll4 SCID mice.

endothelial cell Dll4 and tumor cell–expressed Notch receptors, which could contribute to some of the observed variability in response to Dll4 blockade. Analysis of Notch receptor expression by flow cytometry and Western blot analysis demonstrated Notch receptor expression in 4 of 5 ovarian xenograft cell lines, with only OV90 cells staining negatively for all four Notch receptors. Notch1 was found to be prominently expressed in the ovarian cell lines, whereas Notch2, Notch3, and Notch4 expression was more variable (Fig. 4A; Supplementary Fig. S5A). Immunofluorescence staining confirmed tumor cell expression of Notch1, in addition to its expression in the tumor vasculature, in ovarian xenograft tumors (Fig. 4B; Supplementary Fig. S5B).

To interrogate Notch signaling in ovarian cell lines, we engineered TOV-112D cells to express the RBPj-luciferase Notch signaling reporter. Notch reporter assays demonstrated activation of Notch signaling by both exogenous human and mouse Dll4 protein in TOV-112D cells (Fig. 4C). As expected, Notch signaling activation could be suppressed by treatment with the respective human and mouse Dll4-specific blocking antibodies (Fig. 4C). To determine which Notch receptors mediate the Dll4-dependent activation of the RBPj reporter in TOV-112D cells, we evaluated Notch1- and Notch3-specific function-blocking antibodies. Notch1 antibody treatment partially suppressed RBPj-Notch reporter activation (71% inhibition), whereas the targeting of

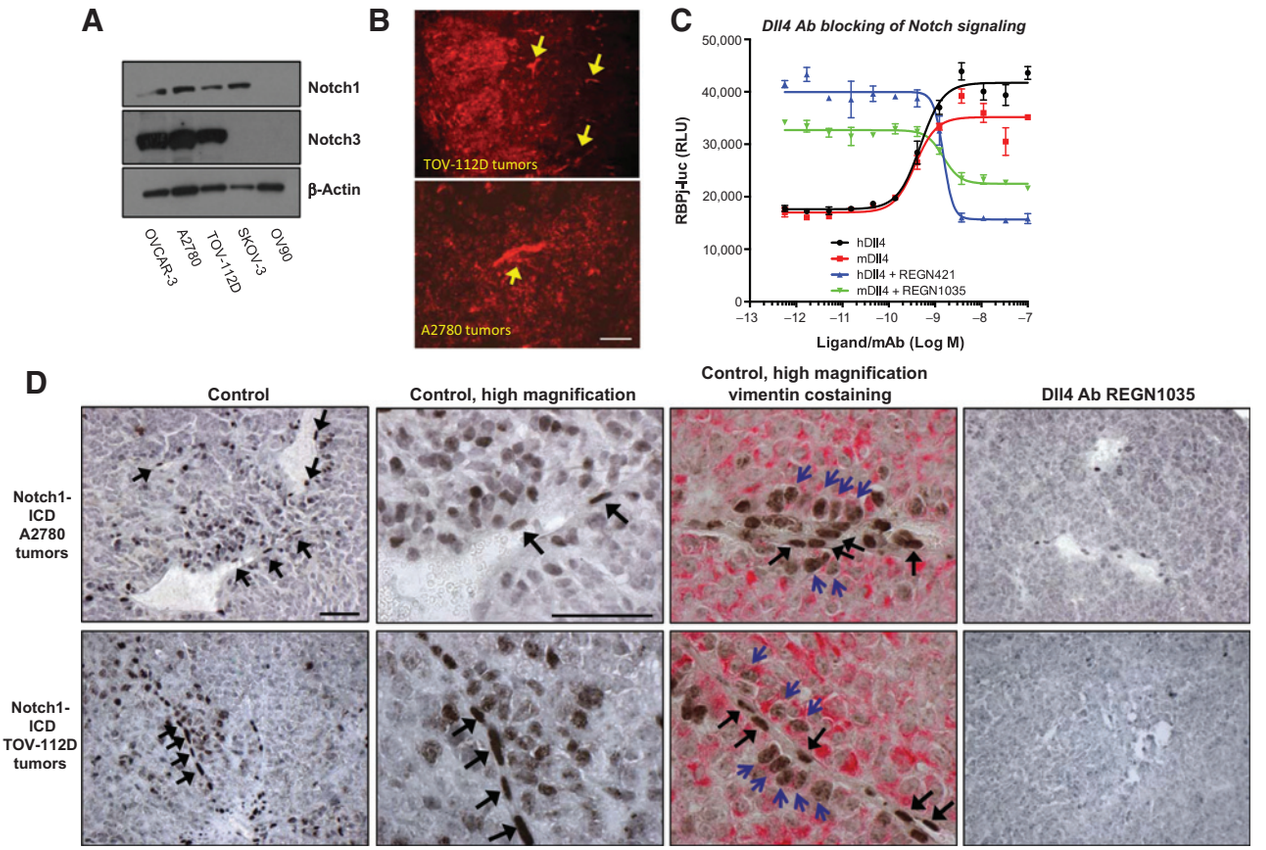

Figure 4.
Paracrine Dll4-Notch signaling in ovarian xenograft tumors. A, Western blot analysis of Notch1 and Notch3 receptor expression in ovarian xenograft cell lines. B, immunofluorescence staining for Notch1 of TOV-112 and A2780 tumors demonstrates Notch1 expression in the tumor parenchyma and in tumor vessels (arrows) C, Notch signaling activation was assessed in TOV-112D cells stably expressing a RBPj-luciferase reporter. EC_{50} for human and mouse Dll4 were determined as 0.5 nmol/L and 0.4 nmol/L, respectively. For inhibition assays, Dll4 was coated onto plates at 11 nmol/L. Dll4 antibodies at indicated doses were preincubated with TOV112D/RBPj-luc cells prior to plate addition. IC_{50} for REGN421 and REGN1035 are 1.5 nmol/L. D, Notch1-ICD staining of sections from A2780 and TOV-112D tumors treated with hFc control protein or REGN1035 (5 mg/kg) for 24 hours. Middle panels display representative high magnification images of hFc control tumor sections stained for Notch1-ICD alone or costained for human vimentin. Black arrows identify elongated Notch1-ICD–positive endothelial cell nuclei, whereas blue arrows highlight vimentin/Notch1-ICD double positive ovarian tumor cells. Scale bars, 50 μm.

Notch 3 did not appreciably affect RBPj reporter activation (Supplementary Fig. S6). Thus, Notch1 but not the putative ovarian cancer oncogene Notch3 appears to be a major mediator of Notch signaling in TOV-112D cells. We next evaluated Notch1 signaling activity in ovarian xenograft tumors *in vivo* by immunohistochemical staining for Notch1 intracellular domain (N1-ICD). Staining of A2780 and TOV-112D tumors demonstrated strong nuclear expression and thus active Notch1 signaling in endothelial cells of tumor vessels (Fig. 4D). In addition, N1-ICD expression was also frequently detected in the tumor parenchyma immediately adjacent to N1-ICD$^+$ endothelial cells (Fig. 4D), a pattern consistent with spatially restricted, paracrine signaling interactions between membrane-tethered endothelial Dll4 and Notch1 receptor expressed by ovarian tumor cells. Tumor cell identity of the N1-ICD$^+$ cells adjacent to tumor vessels with active Notch1 signaling was confirmed by costaining for human vimentin (Fig. 4D).

To evaluate the effects of acute blockade of stromal Dll4 on Notch1 signaling, ovarian tumor–bearing mice were treated with REGN1035 (specific for murine Dll4) for 24 hours, and tumors were analyzed for N1-ICD levels. REGN1035 treatment resulted in a marked reduction of nuclear N1-ICD immunostaining in endothelial cells, indicating the suppression of endothelial Dll4-Notch1 signaling (Fig. 4D). In addition, stromal targeting of Dll4 also reduced Notch1 activity in tumor cells that surrounded the tumor vasculature (Fig. 4D), indicating that the blockade of endothelial Dll4 also disrupts juxtacrine Dll4-Notch1 signaling interactions.

Combinatorial blockade of Dll4 and VEGF signaling results in enhanced ovarian tumor growth inhibition

VEGF-directed targeted therapy has shown clinical benefit and has recently been approved as a treatment modality in ovarian cancer (32). Therefore, we tested whether the blockade of Dll4-Notch combined with VEGF blockade could enhance antitumor efficacy in ovarian xenograft models. Intraperitoneal A2780-tumor bearing SCID mice were treated with REGN1035, the VEGF blocker aflibercept (ziv-aflibercept in the United States; commonly known in the literature as VEGF Trap; ref. 33), or the combination thereof starting 1 week after tumor cell implantation (early treatment regimen) for a total of 4 weeks.

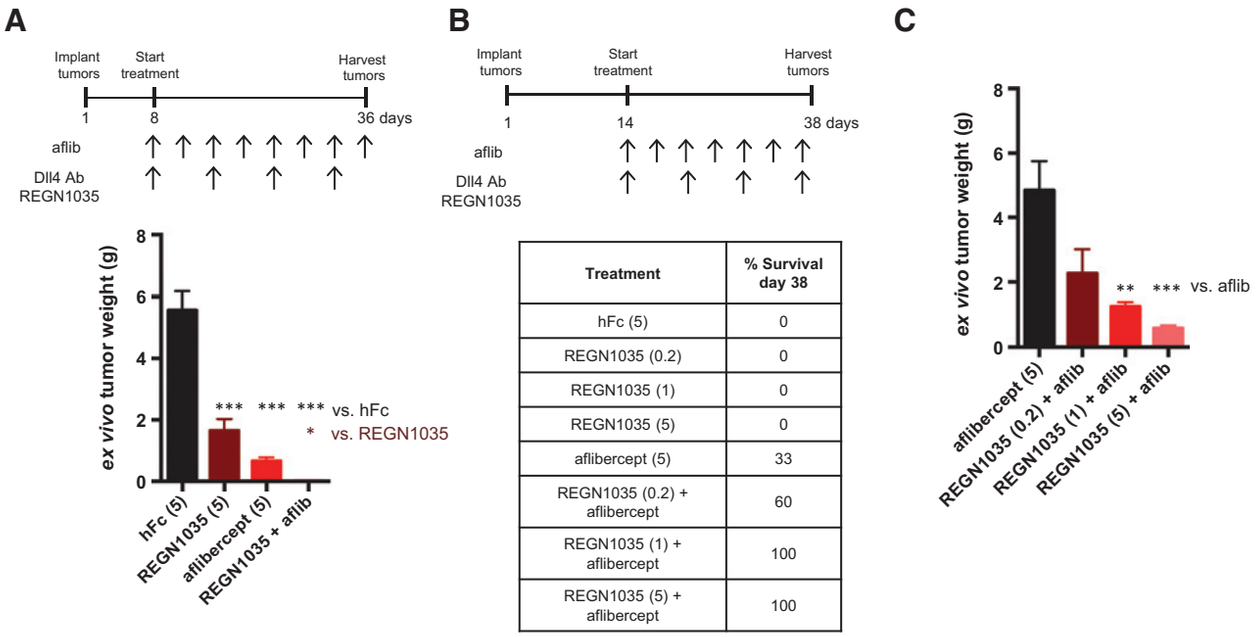

Treatment	% Survival day 38
hFc (5)	0
REGN1035 (0.2)	0
REGN1035 (1)	0
REGN1035 (5)	0
aflibercept (5)	33
REGN1035 (0.2) + aflibercept	60
REGN1035 (1) + aflibercept	100
REGN1035 (5) + aflibercept	100

Figure 5.
Combinatorial blockade of Dll4 and VEGF results in enhanced inhibition of A2780 ovarian tumor growth. A, SCID mice bearing intraperitoneal A2780 tumors were treated with REGN1035, the VEGF blocker aflibercept, or the combination thereof at the indicated doses (mg/kg) starting 1 week after tumor cell implantation for a total of 4 weeks. Treatment regimen is outlined in the scheme at the top; arrows indicate dosing. The bar graphs represent end of study *ex vivo* tumor weight. B, table summarizing survival frequency of A2780-bearing SCID mice treated with the indicated reagents (mg/kg) on day 38 after tumor cell implantation. Treatment was initiated 2 weeks after tumor cell implantation; treatment regimen is outlined in the scheme at the top. C, analysis of *ex vivo* tumor weight of SCID mice bearing intraperitoneal A2780 tumors on day 38 after tumor cell implantation following the treatment paradigm from B. Error bars represent SEM. Treatment groups were compared by one-way ANOVA with Bonferroni multiple comparison test (*, $P < 0.05$; **, $P < 0.01$; ***, $P < 0.001$).

Ex vivo A2780 tumor weight was determined at the end of treatment. Both REGN1035 (5 mg/kg, 1×/week) and aflibercept (5 mg/kg, 2×/week) exhibited potent antitumor effects as single agents in this regimen, producing 70% and 88% TGI, respectively (Fig. 5A). Notably, combined treatment with REGN1035 and aflibercept resulted in enhanced antitumor effects (97% TGI) and virtually complete suppression of intraperitoneal A2780 tumor growth (Fig. 5A). In a late treatment regimen, treatment of A2780 tumor-bearing mice was initiated 2 weeks after tumor cell inoculation. Mice were treated with aflibercept (5 mg/kg, 2×/week), REGN1035 at fully effective dose of 5 mg/kg, and suboptimal doses of 1 mg/kg and 0.2 mg/kg, all administered 1×/week as well as with the respective combinations. Animals in the control and the REGN1035 single-agent treatment groups died or were terminated early due to excessive tumor burden, although REGN1035 showed dose-dependent antitumor activity (Supplementary Table S2). Single-agent aflibercept and combination therapy treatment groups were analyzed on day 38 after tumor cell implantation. Although significant mortality was observed in the aflibercept alone and the 0.2 mg/kg REGN1035 plus aflibercept treatment groups (33% and 60% survival, respectively), survival rates for the 1 mg/kg and 5 mg/kg REGN1035/aflibercept combination groups at day 38 were 100% (Fig. 5B). Analysis of intraperitoneal tumor burden at day 38 confirmed that combined administration of REGN1035 and aflibercept resulted in significantly enhanced inhibition of A2780 tumor growth relative to the single-agent aflibercept control (Fig. 5C). Importantly, survival benefits and enhanced inhibition of A2780 tumor growth of the REGN1035/aflibercept combinations were found to be dose-dependent and were also observed when suboptimal 1 mg/kg doses of REGN1035 were administered in combination with aflibercept (Fig. 5B and C).

Combinatorial blockade of Dll4 and VEGF reverses normal organ vascular changes induced by Dll4 blockade alone

Published reports suggest that chronic blockade of Dll4 results in pathologic activation of endothelial cells and vascular tumorigenesis in select organs (34, 35). Thus, we examined normal organs from adult humanized Dll4 SCID mice treated with REGN421 at fully effective dose of 2.5 mg/kg, given once weekly for a total of 3 weeks by histologic and immunohistochemical analysis. Treatment with REGN421 induced reversible vascular changes selectively in heart and liver of humanized Dll4 SCID mice but not in other organs (lung, kidney, kidney-associated adipose tissue, jejunum, stomach, pancreas, skeletal muscle, spleen, skin, retina). Vascular beds of hearts from REGN421-treated mice exhibited increased vascularity relative to hFc control, as assessed by CD31 staining (Fig 6A) as well as an increase in Ki67-positive proliferating cells (Fig. 6B). Costaining for CD31 and Ki67 demonstrated that REGN421-induced proliferation was restricted to endothelial cells (Fig. 6C). REGN421 effects on heart vascularity were found to be dose-dependent. Thus, doses of REGN421 of 1 mg/kg given once weekly did not induce heart endothelial proliferation in humanized Dll4 mice (Fig. 6D).

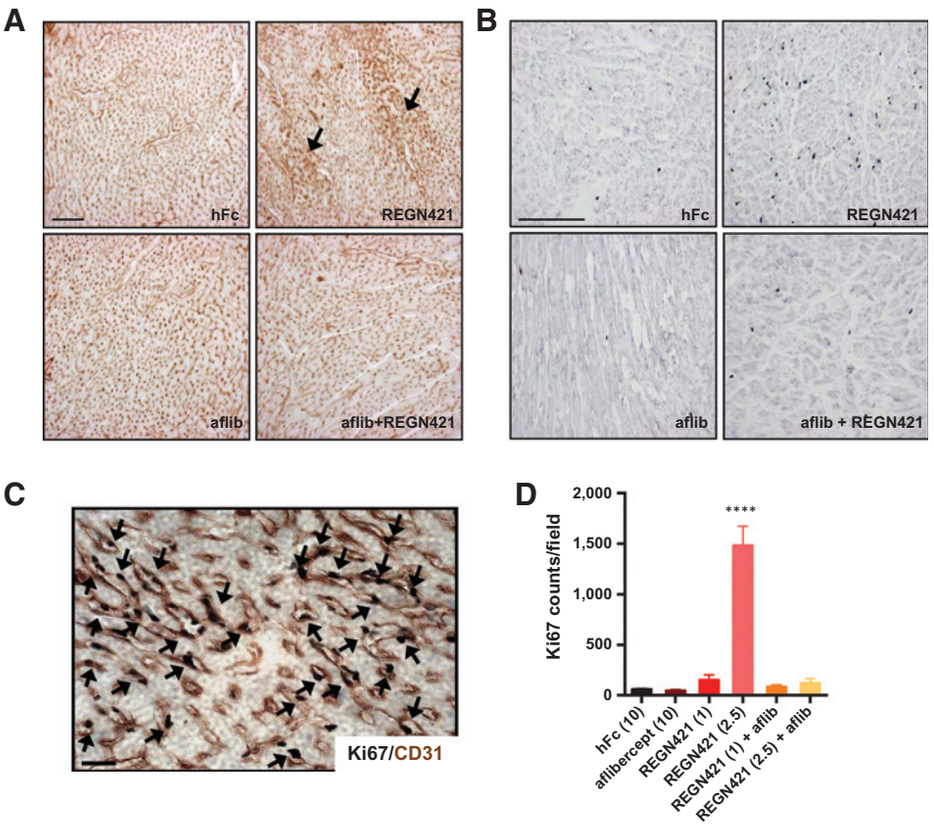

Figure 6.
Combinatorial blockade of Dll4 and VEGF reverses normal organ vascular changes induced by Dll4 blockade alone. A, hearts from humanized Dll4 SCID mice treated with human Fc control (10 mg/kg, twice weekly), REGN421 (2.5 mg/kg, once weekly), VGT (10 mg/kg, twice weekly), or the combination of REGN421 and VGT for 3 weeks were analyzed by CD31 staining. Arrows, areas of increased vascularity. B, heart cellular proliferation was analyzed by Ki67 staining. C, costaining of a heart section from an REGN421-treated animal for CD31 (brown) and Ki67 (black) demonstrates that the REGN421-induced cardiac proliferation is restricted to endothelial cells (arrows). D, quantitation of $Ki67^{+}$-proliferating cells in hearts from humanized Dll4 mice treated with the indicated reagents (mg/kg). Error bars represent SEM. Treatment groups were compared by one-way ANOVA with Bonferroni multiple comparison test (****, $P < 0.0001$ vs. all treatment groups). Scale bars in A and B, 20 μm; in C, 10 μm.

Notably, heart vascular changes induced by Dll4 blockade were entirely dependent on VEGF signaling activity. Coadministration of REGN421 and aflibercept (10 mg/kg, twice weekly) quantitatively reversed heart vascular phenotypes induced by REGN421 single-agent treatment (Fig. 6A, B, and D). A similar increase in vascularity and endothelial cell proliferation, as well as mild sinusoidal dilations, was observed in livers from REGN421-treated mice (Supplementary Fig. S7). Again, liver vascular changes were found to be reversible upon cessation of treatment, dose-dependent, and could be blocked by the simultaneous targeting of VEGF (Supplementary Fig. S7). Vascular phenotypes in response to REGN421 treatment in heart and liver correlated with Dll4 expression and Dll4-dependent Notch1 signaling activity in the endothelium of these organs (Supplementary Figs. S8 and S9).

Discussion

In this study, we investigated the antitumor efficacy of Dll4 antagonism and the mechanisms of Dll4-Notch signaling in ovarian tumors using a fully human Dll4 antibody, REGN421. Because REGN421 selectively blocks human but not mouse Dll4, we engineered humanized Dll4 mice to enable preclinical studies. In addition, we developed selective anti-mouse Dll4 antibodies, allowing us to delineate the relative contributions of blocking stromal versus tumor cell–expressed Dll4. We demonstrated that REGN421 displays potent antitumor activity in several ovarian xenograft models, and that the antitumor activity of blocking Dll4 in ovarian tumors is dependent on targeting stromal, but not tumor cell, Dll4. These findings illustrate the lack of tumor growth-promoting autocrine Dll4-Notch tumor cell signaling in the employed models and are consistent with the relative absence of tumor parenchymal Dll4 expression in the ovarian xenograft tumors. Antitumor activity of targeting host Dll4 was recently also demonstrated in patient-derived renal carcinoma (PDX) models (36).

One would expect tumor cell Dll4 expression and significance of autocrine Dll4-Notch signaling to be tumor model and type specific. Indeed, contributions of autocrine Dll4-Notch signaling to xenograft tumor growth have been described in ovarian and colorectal tumor models (23, 37). Our immunohistological analyses indicate consistent expression of Dll4 in the tumor vasculature, but only sporadic parenchymal expression. These findings are in agreement with reports on Dll4 expression in different human tumor types (18, 19, 21), although one study suggests more widespread Dll4 expression in human ovarian cancer (23). In this latter study, antitumor efficacy for targeting tumor cell–expressed Dll4 was reported (23); however, siRNA approaches were used and may explain the differences in results (38).

In the current study, we provide evidence of paracrine signaling interactions between endothelial cell Dll4 and Notch receptors expressed by adjacent tumor cells. Thus, we detected the selective and Dll4-dependent activation of Notch1 signaling in ovarian tumor cells immediately adjacent to tumor vessels. The functional significance of paracrine Dll4-Notch1 signaling in ovarian tumorigenesis remains to be determined. This question may be addressed preclinically by examining the effects of human Notch1-specific blockers or selective Notch1 knockdown on ovarian xenograft growth. It is conceivable that the spatially restricted paracrine Dll4-Notch1 interactions contribute to the

vascular niche thought to regulate tumor initiating cell maintenance and expansion (37, 39). Conflicting datasets exist as to Notch signaling activity in human ovarian cancer (31, 40). Our data support the careful evaluation of Notch1 signaling activity in human ovarian cancer, in particular in perivascular regions.

The paracrine interactions between membrane-bound endothelial Dll4 ligand and tumor cell–expressed Notch receptors require signaling across the tumor vessel wall. Like normal vessels, tumor vessels are composed of endothelial cells, mural cells, (pericytes or smooth muscle cells) and a basement membrane. In tumor vessels, endothelial cell-pericyte and basement membrane interactions are typically impaired (41), thereby creating opportunities for direct physical interactions between endothelial and tumor cells. We have confirmed that vessels in the ovarian tumor models are only partially covered with pericytes (Supplementary Fig. S10). Furthermore, although one would expect the interactions between the different cell types within the tumor microenvironment to be dynamic, we have identified apparent areas of direct contact between endothelial and tumor cells by confocal microscopy analysis (Supplementary Figs. S10 and S11), a prerequisite for the paracrine Dll4-Notch signaling interactions explored in this article.

We demonstrated in this study that the antitumor activity of Dll4 blockade in ovarian tumors was augmented by the concomitant targeting of VEGF signaling. This finding is consistent with published studies reporting potent combination effects for the simultaneous blockade of Dll4 and VEGF in preclinical models (15, 23, 36). Importantly, we found that the combination benefits of ovarian tumor growth inhibition were dose-dependent and observed even when suboptimal doses of anti-Dll4 antibodies were combined with VEGF blockers. Mechanistically, studies in various model systems have established that Dll4-Notch signaling can provide negative feedback to reduce the activity of the VEGF axis during angiogenic sprouting (4, 5). This model also applies to tumor angiogenesis; however, additional complexities appear to exist in the tumor microenvironment and further investigation is warranted to elucidate the mechanisms of synergy of combined targeting of these two angiogenic signaling systems (42, 43).

Published reports suggest that the chronic blockade of Dll4 results in pathologic activation of endothelial cells and vascular tumorigenesis (35, 44). Similarly, loss of Dll4 or Notch1 function in genetic mouse models led to the activation of liver endothelial cells and the formation of hepatic vascular lesions (34, 45). We have found that prolonged treatment with REGN421 induced vascular changes selectively in heart and liver of humanized Dll4 SCID mice but not in other organs. In particular, we did not observe subcutaneous ulcerative vascular lesions in mice that were previously reported (35) in rats. Similar to what was reported, we found the vascular proliferation to be dose dependent and reversible upon cessation of treatment (35). Importantly, liver and heart vascular changes were dependent on VEGF signaling activity. Collectively, these data suggest that combined blockade of Dll4 and VEGF signaling may increase the therapeutic window for antiangiogenesis-based therapy of ovarian and other solid malignancies.

Overall, this study illustrates the power of using humanized mouse models for the evaluation of non-mouse cross-reactive clinical candidates. REGN421 is currently in a phase I trial (NCT00871559) for patients with advanced solid malignancies (46). The findings presented in this study lend further support for the therapeutic targeting of Dll4 as a promising new antiangiogenesis strategy in ovarian cancer and suggest particular clinical benefit for the blockade of Dll4 with REGN421 in combination with the targeting of VEGF signaling.

Disclosure of Potential Conflicts of Interest

All authors are employees of Regeneron Pharmaceuticals, Inc. G. Thurston has ownership interest (including patents) in patent applications. No potential conflicts of interest were disclosed by the other authors.

Authors' Contributions

Conception and design: F. Kuhnert, J.R. Kirshner, G. Thurston
Development of methodology: F. Kuhnert, G. Chen, S. Coetzee, J. Shan, P. Kovalenko, I. Noguera-Troise, E. Smith, J. Fairhurst, G. Thurston
Acquisition of data (provided animals, acquired and managed patients, provided facilities, etc.): F. Kuhnert, G. Chen, S. Coetzee, N. Thambi, C. Hickey, J. Shan, J. Fairhurst, G. Thurston
Analysis and interpretation of data (e.g., statistical analysis, biostatistics, computational analysis): F. Kuhnert, J. Shan, I. Noguera-Troise, J. Fairhurst, J. Andreev, N. Papadopoulos, G. Thurston
Writing, review, and/or revision of the manuscript: F. Kuhnert, G. Thurston
Study supervision: F. Kuhnert, G. Thurston

Acknowledgments

The authors thank all Regeneron employees that contributed to the generation of REGN421, and provided helpful comments and suggestions.

The costs of publication of this article were defrayed in part by the payment of page charges. This article must therefore be hereby marked *advertisement* in accordance with 18 U.S.C. Section 1734 solely to indicate this fact.

Received December 29, 2014; revised July 10, 2015; accepted July 14, 2015; published OnlineFirst September 16, 2015.

References

1. Artavanis-Tsakonas S, Rand MD, Lake RJ. Notch signaling: cell fate control and signal integration in development. Science 1999;284:770–6.
2. Bray SJ. Notch signalling: a simple pathway becomes complex. Nat Rev Mol Cell Biol 2006;7:678–89.
3. Hofmann JJ, Iruela-Arispe ML. Notch signaling in blood vessels: who is talking to whom about what? Circ Res 2007;100:1556–68.
4. Phng LK, Gerhardt H. Angiogenesis: a team effort coordinated by notch. Dev Cell 2009;16:196–208.
5. Roca C, Adams RH. Regulation of vascular morphogenesis by Notch signaling. Genes Dev 2007;21:2511–24.
6. Hellstrom M, Phng LK, Hofmann JJ, Wallgard E, Coultas L, Lindblom P, et al. Dll4 signalling through Notch1 regulates formation of tip cells during angiogenesis. Nature 2007;445:776–80.
7. Leslie JD, Ariza-McNaughton L, Bermange AL, McAdow R, Johnson SL, Lewis J. Endothelial signalling by the Notch ligand Delta-like 4 restricts angiogenesis. Development 2007;134:839–44.
8. Lobov IB, Renard RA, Papadopoulos N, Gale NW, Thurston G, Yancopoulos GD, et al. Delta-like ligand 4 (Dll4) is induced by VEGF as a negative regulator of angiogenic sprouting. Proc Natl Acad Sci U S A 2007;104:3219–24.
9. Sainson RC, Aoto J, Nakatsu MN, Holderfield M, Conn E, Koller E, et al. Cell-autonomous notch signaling regulates endothelial cell branching and proliferation during vascular tubulogenesis. FASEB J 2005;19:1027–9.
10. Siekmann AF, Lawson ND. Notch signalling limits angiogenic cell behaviour in developing zebrafish arteries. Nature 2007;445:781–4.

11. Suchting S, Freitas C, leNoble F, Benedito R, Breant C, Duarte A, et al. The Notch ligand Delta-like 4 negatively regulates endothelial tip cell formation and vessel branching. Proc Natl Acad Sci U S A 2007;104:3225–30.
12. Tammela T, Zarkada G, Wallgard E, Murtomaki A, Suchting S, Wirzenius M, et al. Blocking VEGFR-3 suppresses angiogenic sprouting and vascular network formation. Nature 2008;454:656–60.
13. Li JL, Sainson RC, Shi W, Leek R, Harrington LS, Preusser M, et al. Delta-like 4 Notch ligand regulates tumor angiogenesis, improves tumor vascular function, and promotes tumor growth in vivo. Cancer Res 2007;67:11244–53.
14. Noguera-Troise I, Daly C, Papadopoulos NJ, Coetzee S, Boland P, Gale NW, et al. Blockade of Dll4 inhibits tumour growth by promoting non-productive angiogenesis. Nature 2006;444:1032–7.
15. Ridgway J, Zhang G, Wu Y, Stawicki S, Liang WC, Chanthery Y, et al. Inhibition of Dll4 signalling inhibits tumour growth by deregulating angiogenesis. Nature 2006;444:1083–7.
16. Scehnet JS, Jiang W, Kumar SR, Krasnoperov V, Trindade A, Benedito R, et al. Inhibition of Dll4-mediated signaling induces proliferation of immature vessels and results in poor tissue perfusion. Blood 2007;109:4753–60.
17. Milano J, McKay J, Dagenais C, Foster-Brown L, Pognan F, Gadient R, et al. Modulation of notch processing by gamma-secretase inhibitors causes intestinal goblet cell metaplasia and induction of genes known to specify gut secretory lineage differentiation. Toxicol Sci 2004;82:341–58.
18. Jubb AM, Soilleux EJ, Turley H, Steers G, Parker A, Low I, et al. Expression of vascular notch ligand delta-like 4 and inflammatory markers in breast cancer. Am J Pathol 2010;176:2019–28.
19. Jubb AM, Turley H, Moeller HC, Steers G, Han C, Li JL, et al. Expression of delta-like ligand 4 (Dll4) and markers of hypoxia in colon cancer. Br J Cancer 2009;101:1749–57.
20. Mailhos C, Modlich U, Lewis J, Harris A, Bicknell R, Ish-Horowicz D. Delta4, an endothelial specific notch ligand expressed at sites of physiological and tumor angiogenesis. Differentiation 2001;69:135–44.
21. Patel NS, Dobbie MS, Rochester M, Steers G, Poulsom R, Le Monnier K, et al. Up-regulation of endothelial delta-like 4 expression correlates with vessel maturation in bladder cancer. Clin Cancer Res 2006;12:4836–44.
22. Patel NS, Li JL, Generali D, Poulsom R, Cranston DW, Harris AL. Up-regulation of delta-like 4 ligand in human tumor vasculature and the role of basal expression in endothelial cell function. Cancer Res 2005;65:8690–7.
23. Hu W, Lu C, Dong HH, Huang J, Shen DY, Stone RL, et al. Biological roles of the Delta family Notch ligand Dll4 in tumor and endothelial cells in ovarian cancer. Cancer Res 2011;71:6030–9.
24. Liu J, Matulonis UA. Anti-angiogenic agents in ovarian cancer: dawn of a new era? Curr Oncol Rep 2011;13:450–8.
25. Jain RK, Duda DG, Clark JW, Loeffler JS. Lessons from phase III clinical trials on anti-VEGF therapy for cancer. Nat Clin Pract Oncol 2006;3:24–40.
26. Casanovas O, Hicklin DJ, Bergers G, Hanahan D. Drug resistance by evasion of antiangiogenic targeting of VEGF signaling in late-stage pancreatic islet tumors. Cancer Cell 2005;8:299–309.
27. Kerbel RS, Yu J, Tran J, Man S, Viloria-Petit A, Klement G, et al. Possible mechanisms of acquired resistance to anti-angiogenic drugs: implications for the use of combination therapy approaches. Cancer Metastasis Rev 2001;20:79–86.
28. Hsieh JJ, Henkel T, Salmon P, Robey E, Peterson MG, Hayward SD. Truncated mammalian Notch1 activates CBF1/RBPJk-repressed genes by a mechanism resembling that of Epstein-Barr virus EBNA2. Mol Cell Biol 1996;16:952–9.
29. Nakatsu MN, Hughes CC. An optimized three-dimensional in vitro model for the analysis of angiogenesis. Methods Enzymol 2008;443:65–82.
30. Nakatsu MN, Sainson RC, Aoto JN, Taylor KL, Aitkenhead M, Perez-del-Pulgar S, et al. Angiogenic sprouting and capillary lumen formation modeled by human umbilical vein endothelial cells (HUVEC) in fibrin gels: the role of fibroblasts and Angiopoietin-1. Microvasc Res 2003;66:102–12.
31. Kluk MJ, Ashworth T, Wang H, Knoechel B, Mason EF, Morgan EA, et al. Gauging NOTCH1 activation in cancer using immunohistochemistry. PLoS One 2013;8:e67306.
32. Pujade-Lauraine E, Hilpert F, Weber B, Reuss A, Poveda A, Kristensen G, et al. Bevacizumab combined with chemotherapy for platinum-resistant recurrent ovarian cancer: The AURELIA open-label randomized phase III trial. J Clin Oncol 2014;32:1302–8.
33. Hu L, Hofmann J, Holash J, Yancopoulos GD, Sood AK, Jaffe RB. Vascular endothelial growth factor trap combined with paclitaxel strikingly inhibits tumor and ascites, prolonging survival in a human ovarian cancer model. Clin Cancer Res 2005;11:6966–71.
34. Liu Z, Turkoz A, Jackson EN, Corbo JC, Engelbach JA, Garbow JR, et al. Notch1 loss of heterozygosity causes vascular tumors and lethal hemorrhage in mice. J Clin Invest 2011;121:800–8.
35. Yan M, Callahan CA, Beyer JC, Allamneni KP, Zhang G, Ridgway JB, et al. Chronic DLL4 blockade induces vascular neoplasms. Nature 2010;463:E6–7.
36. Miles KM, Seshadri M, Ciamporcero E, Adelaiye R, Gillard B, Sotomayor P, et al. Dll4 blockade potentiates the anti-tumor effects of VEGF inhibition in renal cell carcinoma patient-derived xenografts. PLoS One 2014;9:e112371.
37. Hoey T, Yen WC, Axelrod F, Basi J, Donigian L, Dylla S, et al. DLL4 blockade inhibits tumor growth and reduces tumor-initiating cell frequency. Cell Stem Cell 2009;5:168–77.
38. Kaelin WG Jr. Molecular biology. Use and abuse of RNAi to study mammalian gene function. Science 2012;337:421–2.
39. Butler JM, Kobayashi H, Rafii S. Instructive role of the vascular niche in promoting tumour growth and tissue repair by angiocrine factors. Nat Rev Cancer 2010;10:138–46.
40. Rose SL, Kunnimalaiyaan M, Drenzek J, Seiler N. Notch 1 signaling is active in ovarian cancer. Gynecol Oncol 2010;117:130–3.
41. Baluk P, Hashizume H, McDonald DM. Cellular abnormalities of blood vessels as targets in cancer. Curr Opin Genet Dev 2005;15:102–11.
42. Li JL, Sainson RC, Oon CE, Turley H, Leek R, Sheldon H, et al. DLL4-Notch signaling mediates tumor resistance to anti-VEGF therapy in vivo. Cancer Res 2011;71:6073–83.
43. Thurston G, Kitajewski J. VEGF and Delta-Notch: interacting signalling pathways in tumour angiogenesis. Br J Cancer 2008;99:1204–9.
44. Li JL, Jubb AM, Harris AL. Targeting DLL4 in tumors shows preclinical activity but potentially significant toxicity. Future Oncol 2010;6:1099–103.
45. Djokovic D, Trindade A, Gigante J, Badenes M, Silva L, Liu R, et al. Combination of Dll4/Notch and Ephrin-B2/EphB4 targeted therapy is highly effective in disrupting tumor angiogenesis. BMC Cancer 2010;10:641.
46. Chiorean EG, LoRusso P, Strother RM, Diamond JR, Younger A, Messersmith WA, et al. A phase I first-in-human study of Enoticumab (REGN421), a Fully Human Delta-like Ligand 4 (Dll4) monoclonal antibody in patients with advanced solid tumors. Clin Cancer Res 2015;21:2695–703.